Profiling translatomes of discrete cell populations resolves altered cellular priorities during hypoxia in *Arabidopsis*

Angelika Mustroph[a], M. Eugenia Zanetti[a,1], Charles J. H. Jang[a], Hans E. Holtan[b], Peter P. Repetti[b], David W. Galbraith[c], Thomas Girke[a], and Julia Bailey-Serres[a,2]

[a]Center for Plant Cell Biology and Department of Botany and Plant Sciences, Batchelor Hall, University of California, Riverside, CA 92521; [b]Mendel Biotechnology, Inc., 3935 Point Eden Way, Hayward, CA 94545; and [c]Department of Plant Sciences, University of Arizona, 1140 E. South Campus Drive, Forbes Building, Room 303, Tucson, AZ 85721

Multicellular organs are composed of distinct cell types with unique assemblages of translated mRNAs. Here, ribosome-associated mRNAs were immunopurified from specific cell populations of intact seedlings using *Arabidopsis thaliana* lines expressing a FLAG-epitope tagged ribosomal protein L18 (FLAG-RPL18) via developmentally regulated promoters. The profiling of mRNAs in ribosome complexes, referred to as the translatome, identified differentially expressed mRNAs in 21 cell populations defined by cell-specific expression of FLAG-RPL18. Phloem companion cells of the root and shoot had the most distinctive translatomes. When seedlings were exposed to a brief period of hypoxia, a pronounced reprioritization of mRNA enrichment in the cell-specific translatomes occurred, including a ubiquitous rise in 49 mRNAs encoding transcription factors, signaling proteins, anaerobic metabolism enzymes, and uncharacterized proteins. Translatome profiling also exposed an intricate molecular signature of transcription factor (TF) family member mRNAs that was markedly reconfigured by hypoxia at global and cell-specific levels. In addition to the demonstration of the complexity and plasticity of cell-specific populations of ribosome-associated mRNAs, this study provides an in silico dataset for recognition of differentially expressed genes at the cell-, region-, and organ-specific levels.

Plants are endowed with remarkable flexibility in gene expression that modulates metabolism and development in response to a wide variety of environmental cues. But multicellularity limits the assessment of alterations in gene regulation within individual cell types that orchestrate the organ to whole-plant adjustments that are critical for acclimation and adaptation. The mRNAs of cells of distinct identity can be isolated by microdissection of tissues or sorting of protoplasts marked by the expression of green fluorescent protein (GFP) (1–5). The profiling of total cellular mRNAs obtained from sorted protoplasts of root cell types from *Arabidopsis thaliana* exposed to nitrogen or perturbed by iron and sodium chloride demonstrated that environment plays a role in decisions regarding cell identity (6, 7). Such refined knowledge of cell-type specific patterns of gene expression is crucial for the resolution of gene networks associated with development and stress responses. These methods, however, are limited to one particular aspect of gene expression, specifically that measured in terms of total transcript abundance, and are only valid for networks that are unperturbed during cell isolation.

Standard procedures for extraction of mRNA from organs not only disrupt cell-specific gene expression but obscure the partitioning of mRNAs into ribonucleoprotein (mRNP) complexes of distinct function, such as polyribosomes (polysomes) and mRNPs that mediate transport, localization, storage, or degradation (8, 9). This is relevant in plants and other eukaryotes because the formation of mRNA-ribosome complexes is a selective process and can be dramatically reprioritized when homeostasis is perturbed (10–13). Even in the absence of stress the process of translation is primarily controlled during the recruitment of the 43S preinitiation complex to the mRNA (9). Therefore, mRNAs in polysomes are actively translated, although a minor subpopulation of these may be stalled in initiation or elongation as a result of miRNA-mediated repression or another mechanism (14, 15). Because of this, profiling total cellular mRNAs provides less insight into the cellular state than mRNAs in ribosome complexes.

We previously reported the efficient immunopurification of mRNAs in ribosome complexes, the subpopulation of mRNAs referred to as the translatome (16), by use of a FLAG-tagged ribosomal protein L18 (RPL18) in *Arabidopsis* (17). This noninvasive strategy enabled an integrated analysis of transcriptomic, translatomic, and metabolic adjustments to hypoxia and reoxygenation in whole seedlings (13). Epitope-tagged ribosomes were similarly captured to assess the remodeling of the translatome of yeast following mild and severe stress (16), and in discrete cell types in heterogeneous cultures of mouse neuronal cells (18). Here, the immunopurification of mRNA-ribosome complexes was extended by using developmentally regulated promoters to drive FLAG-RPL18, allowing the generation of an atlas of the translated mRNAs within 21 specific cell populations of the seedlings. We also explored global and cell-specific adjustments of 19 cell-specific translatomes in response to hypoxia. This strategy provided unprecedented resolution of mRNA content and enrichment in distinct cell populations of photosynthetic and nonphotosynthetic organs of seedlings, and can be readily extended to other cells and developmental stages.

Results and Discussion

Immunopurification and Profiling of Ribosome-Associated mRNAs from Specific Cell Populations. Our goal was to establish a robust method for measurement of ribosome-associated mRNAs within cells of distinct identity that could be used to monitor rapid remodeling of gene expression in response to specific stimuli, such as stresses or small molecules. A criterion was that ephemeral changes in gene expression could be quantified for both root and shoot cell types of varying abundance. This was accomplished by use of 13 promoters to direct regional and cell-type specific expression of FLAG-tagged RPL18 (Table 1; Fig. 1; Fig. S1 in *SI Appendix*),

Table 1. Summary of regions and cell types targeted with *promoter:FLAG-RPL18* lines established in *Arabidopsis thaliana* (*Col-0*)

Target cell type	Promoter
Near constitutive	Cauliflower mosaic virus 35S (*p35S*)
Root proliferating cells	Ribosomal protein L11C (*pRPL11C*)
Root endodermis, quiescent center	SCARECROW (*pSCR*)
Root vasculature	SHORTROOT (*pSHR*)
Root vasculature	WOODENLEG (*pWOL*)
Root and shoot phloem companion cells	Sucrose transporter2 (*pSUC2*)
Root phloem companion cells, shoot bundle sheath	Sulfate transporter (*pSULTR2;2*)
Root atrichoblast epidermis, shoot trichomes*	GLABRA2 (*pGL2*)
Root cortex meristematic zone	Cortex specific transcript (*pCO2*)
Root cortex elongation and maturation zone	Endopeptidase (*pPEP*)
Shoot photosynthetic	Rubisco small subunit (*pRBCS1A*)
Cotyledon and leaf epidermis	Cuticular wax gene (*pCER5*)
Cotyledon and leaf guard cells	K$^+$ channel (*pKAT1*)

*, *pGL2* was expressed in the targeted cell type and in the root phloem companion cells.

shown previously to assemble into functional 80S ribosomes and polysomes that can be efficiently immunoprecipitated from lysates of cryopreserved tissue (13, 17). The extension of the ribosome immunopurification method to specific cell populations was validated by quantitative comparison of the cohort mRNAs captured from roots of two independent *pGL2:FLAG-RPL18* lines ($r^2 >$ 0.98), which was found to be as reproducible as immunopurification of mRNAs from biological replicate samples ($r^2 > 0.97$) (Fig. S2 in *SI Appendix*). We anticipated that the mRNAs immunopurified from *p:FLAG-RPL18* lines would correspond to the spatial and temporal expression of the promoter-driving RPL18 expression and used multiple promoters to target some cell types at different stages of development (i.e., stele, *pWOL*, and *pSHR*; cortex, *pCO2*, and

Fig. 1. Promoters used in this study. Individual promoters were used to drive the production of FLAG-GFP-RPL18 in transgenic *Arabidopsis* seedlings (Table 1). Representative images demonstrate the specificity of promoter activity in 7-d-old seedlings of T2 transgenics expressing FLAG-GFP-RPL18. Green, GFP fluorescence; red, chlorophyll in shoots, propidium iodide staining in roots; QC, quiescent center; LR, lateral root primordia. (Scale bar, 50 μm.)

pPEP; phloem companion cells (CC), *pSUC2* and *pSULTR2;2*). To confirm promoter activity, we produced independent transgenics for each promoter-driving *FLAG-GFP-RPL18* and confirmed the accumulation of GFP in the targeted cell types (Fig. S1 *A–C* in *SI Appendix*). As expected, GFP-RPL18 accumulated in nucleoli and was dispersed in the cytosol (Fig. S1*D* in *SI Appendix*). For each *p:FLAG-RPL18* line, the T-DNA insertion site, sedimentation of FLAG-tagged ribosome complexes, and growth was monitored (*SI Appendix*). All lines displayed normal development and fecundity.

Thirteen *p:FLAG-RPL18* lines were used to immunopurify mRNA-ribosome complexes of the root tip (apical 1 cm, including the meristematic and elongation zones), whole root, and shoot of 7-d-old seedlings cultured in the presence (control, C) or absence of air (2-h hypoxia, H) (Table 1; Table S1 and Fig. S3 in *SI Appendix*). Forty translatomes were evaluated, along with six transcriptomes of the *35S:FLAG-RPL18* line. Levels of mRNAs were highly correlated across biological replicates representing organ or cell population and treatment samples ($r^2 = 0.93$–0.99). Altogether, expression data were obtained for 17,642 genes (probe sets) with signal levels above the detection limit in at least one of the 46 samples (Dataset S1). A cohort of 6,500 mRNAs was detected in all samples (37% of all detected mRNAs) (Dataset S1, sheet *b*). The data for individual Arabidopsis mRNAs can be viewed schematically at the organ-, region-, and cell-specific levels via the electronic fluorescent protein (eFP) platform (19) (Fig. S4 in *SI Appendix*).

Characterization of Translatomes of Specific Cell Populations. Differentially expressed genes (DEGs) were identified by comparison of the robust multichip average (RMA) normalized signal values for one cell population (i.e., endodermal-expressed *pSCR:FLAG-RPL18*) to the signal from nonoverlapping cell populations of the same organ (i.e., pWOL, *pSHR*, *pGL2*, *pSUC2*, *pSULTR2;2*, *pPEP*, or *pCO2*). For some of the targeted cell types, multiple stringencies of comparison were applied for robust identification of mRNAs enriched in a cell population (Dataset S2, sheet *b*). All translatomes examined had DEGs, defined as mRNAs that were significantly enriched or depleted relative to other cell-specific populations of the same organ (>2-fold change, FDR < 0.01) (Dataset S2). The number of significantly enriched mRNAs in the root samples ranged from 27 in the cortex meristem (*pCO2*) to 480 in phloem CC (*pSUC2*). In the shoot, the *pSUC2* mRNA population was also the most distinct, with 798 enriched transcripts in contrast to 20 mRNAs in the trichome-targeted (*pGL2*) population.

To aid recognition of coordinately regulated transcripts, fuzzy *k*-means clustering was performed on the RMA normalized signal data. This resolved 59 clusters of mRNAs that were coregulated at the organ-, region-, and cell-specific levels (Fig. 2*A*; Dataset S3; Fig. S5 in *SI Appendix*). The assessment of enriched gene ontology (GO) terms within the DEGs of individual translatomes (Dataset S2; Fig. S6 in *SI Appendix*) and fuzzy *k*-means clusters (Dataset S3; Fig. S5*B* in *SI Appendix*) confirmed significant biases in abundance of mRNAs encoding proteins associated with specialized functions and processes in each translatome. To further validate the capture of mRNAs from the targeted cell populations we compared cell-specific transcriptome data obtained by microdissection or sorting of GFP-labeled protoplasts to the translatomes (Fig. 2*B*; Dataset S4; Dataset S2; Fig. S7 in *SI Appendix*). In all cases, overlap was observed between transcriptomes and translatomes of a targeted cell type. Reasons for incomplete overlap between cell-specific mRNA populations obtained by different methods are manifold. First of all, transcriptomes and translatomes are nonidentical because only a portion of a gene's transcripts are associated with ribosomes as a result of selective translational initiation (10–13, 17). Additionally, differences may be attributed to distinctions in growth conditions, developmental age, time of harvest, promoter activity, and sample manipulation in the independent studies.

The translatomes obtained from phloem CC populations exemplify the results obtained by the ribosome immunopurification
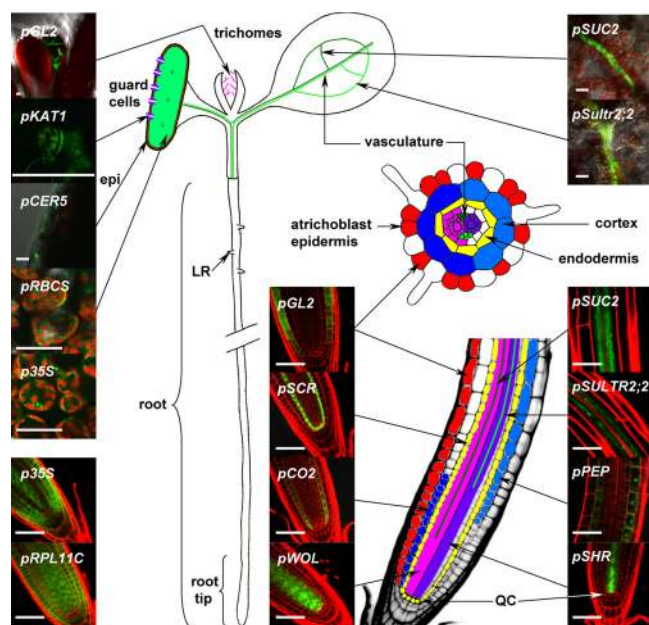
Mustroph et al.

Fig. 2. Cell-specific expression patterns across organs. (*A*) RMA-normalized data of 11,273 genes (probe pair sets) from control-grown plants were analyzed by fuzzy *k*-means clustering to identify coregulated genes in translatomes of different cell populations. The median log₂ expression value of the 59 clusters was calculated from scaled values. Each cluster includes genes with a similar enrichment/depletion pattern across samples. Clusters were sorted by expression maxima of samples to visualize trends in mRNA enrichment. Sample names correspond to promoters driving *FLAG-RPL18* expression (Table 1). RT, root tip; R, root; S, shoot; PCC, phloem CC. (*Right*) Selected cluster probe set data and enriched gene ontology (GO) categories (*P*-values calculated by GOHyperGAll, see ref. 32). (*B*) Identification of 214 phloem CC-enriched mRNAs across organs and experiments (Dataset S4, sheet e). DEGs of *pSUC2* root and shoot translatomes (Dataset S2, sheet a) and *pSUC2:GFP* protoplasts (4). Fig. S5 in *SI Appendix* shows an expanded panel *A* and additional clusters.

PLANT BIOLOGY

strategy. *pSUC2:GFP-RPL18* was expressed in CC of the entire root whereas *pSULTR2;2:GFP-RPL18* was limited to CC of the elongation and maturation region (Fig. S1*C* in *SI Appendix*). Consistent with the regional distinctions in expression of these promoters, the *pSUC2* and *pSULTR2;2* root translatomes were highly overlapping but nonidentical (Dataset S2; Fig. S8 in *SI Appendix*). The 270 coenriched transcripts included a number of phloem CC markers [i.e., *SUC2*, Sucrose-H⁺ symporter (At1g22710); *AHA3*, plasma membrane H⁺ ATPase (At5g57350); *APL*, G2-type transcription factor (TF) associated with phloem development (At1g79430); two phloem-specific lectins (At4g19840 and At2g02230)], supporting the conclusion that mRNAs were effectively isolated from the targeted cell type. Fuzzy *k*-means clustering sorted the root-enriched phloem CC mRNAs into three groups (clusters 22, 23, and 30) (Fig. 2*A*). Unexpectedly, root *pGL2* mRNAs were also enriched in these clusters. We subsequently confirmed that *pGL2:GFP-RPL18* lines accumulate low levels of GFP-RPL18 in the root phloem CC (Fig. S1*B* in *SI Appendix*), indicating that the *pGL2* translatome was not limited to the intended cell type (root atrichoblasts). In the seedling shoot, both *pSUC2:GFP-RPL18* and *pSULTR2;2:GFP-RPL18* were expressed in the vasculature. However, six dominant clusters (1, 5, 6, 22, 34, and 51), representing 1,094 significantly shoot-enriched mRNAs, were predominantly limited to the *pSUC2* translatome (Fig. 2*A*; Dataset S3; Fig. S5*B* in *SI Appendix*). By contrast, the shoot *pSULTR2;2* mRNA population included significant levels of photosynthesis-related mRNAs (cluster 7), consistent with the reported activity of this promoter in shoot bundle sheath cells (20). We also compared the shoot and root *pSUC2* translatomes with mRNAs obtained from *pSUC2:GFP* protoplasts of seedling roots (4). This identified 214 enriched mRNAs present in all 3 samples (Fig. 2*B*; Dataset S4), including sucrose and amino acid transporters and proteins involved in redox control. Notably, the shoot *pSUC2*-enriched mRNAs included 81 TFs (i.e., cluster 6, 2.50*E*-03) (Dataset S2 and S3) and genes involved in floral determination (i.e., CONSTANS, At5g15840;

FLOWERING LOCUS C, At5g10140; floral homeotic protein AGL9, At1g24260). Remarkably, 78 of the reported phloem sap mRNAs were markedly enriched in the shoot *pSUC2* translatome (Fig. S7*C* in *SI Appendix*). Together with the observation that the phloem transcriptome includes mobile mRNAs (21) and its proteome includes many ribosomal proteins (22), this observation raises the possibility that ribosomes function in long-distance mRNA trafficking.

Additional cell types of the shoot were effectively targeted with *pRBCS* (photosynthetic cells), *pCER5* (epidermal cells), and *pKAT1* (guard cells). Consistent with expectations, *pRBCS* mRNAs were highly enriched for proteins involved in all aspects of photosynthesis (Fig. 2*A*, cluster 7; Dataset S3). These mRNAs were abundant in guard cells (*pKAT1*), depleted from the shoot phloem CC (*pSUC2*) and epidermis (*pCER5*), and largely absent from root mRNAs. The pCER5 epidermis-enriched mRNAs encoded proteins involved in cuticle development (1.21*E*-05), cell-wall modification (2.88*E*-03), fatty acid biosynthesis (6.81*E*-10) (Fig. 2*A*, cluster 16), and included epidermal markers [*BODYGUARD* (At1g64670); L1-specific homeobox protein *AtML1* (At4g21750)]. mRNAs of the epidermis-enriched cluster 16 were also associated with hormonal responses, including jasmonate (2.66*E*-03), auxin (1.12*E*-08), gibberellin (1.37*E*-02), and salicylic acid (8.16*E*-03) (Dataset S3; Fig. S5*B* in *SI Appendix*). The guard cell-enriched (*pKAT1*) mRNAs sorted into three major groups (clusters 27, 50, and 54) (Fig. 2*A*; Dataset S3), which included guard cell marker [*SLAC1*, slow anion gated channel (At1g12480); a putative Na⁺/K⁺ antiporter (At3g53720); *KEA1*, K⁺ efflux antiporter (At1g01790); putative protein kinases (At4g33950 and At1g62400); protein phosphatase 2A beta (At3g09880 and At5g03470)]. Appropriately, *pKAT1*-enriched TFs (cluster 54) included FAMA (At3g24140), a basic helix–loop–helix TF required for terminal guard cell differentiation (23) and At-MYB60 (At1g08810), involved in ABA-mediated stomatal activity (24). The pronounced enrichment of mRNAs associated with guard cell morphogenesis and activity in the *pCER5* and *pKAT1* popula-
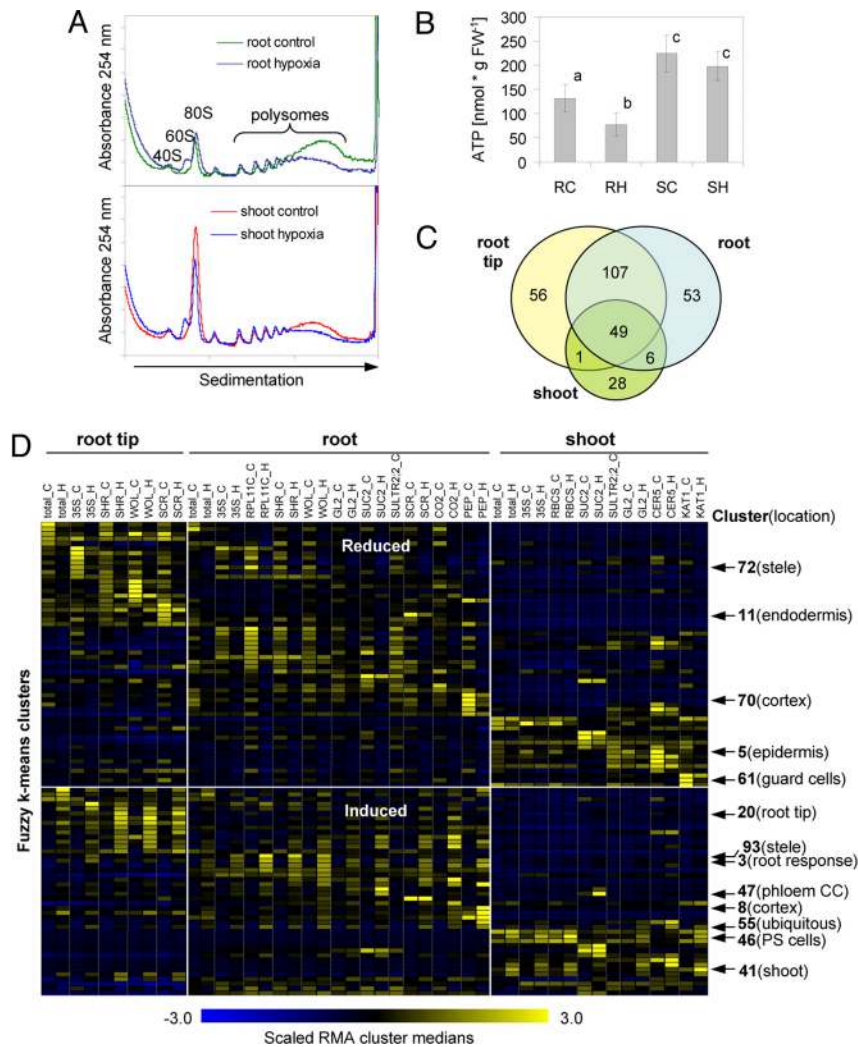
Fig. 3. Hypoxia triggers global, organ-, and cell-specific responses. (*A*) Polysomes decrease more dramatically in roots than shoots when 7-d-old seedlings are hypoxic for 2 h. Absorbance profile of sucrose density gradient fractionated polysomes. (*B*) Mean ATP content of samples used in polysome analysis ± SD. (*n* = 5), letters indicate significantly different values (*P* < 0.05 of 2-sided *t* test). RC, root control; RH, root hypoxia; SC, shoot control; SH, shoot hypoxia. (*C*) Overlap in mRNAs with a significant increase in translatomes of cells sampled in an organ or region after 2-h hypoxia (SLR > 1, FDR < 0.01). (*D*) Response to hypoxia includes increases and decreases in mRNAs of cell-specific translatomes. Fuzzy *k*-means clustering of 6,461 genes (probe pair sets) with a significant change (Dataset S6). For each cluster, the median of scaled RMA normalized data is shown. Clusters were sorted by expression maxima for each mRNA population. Horizontal white line separates hypoxia-repressed (*Upper*) and hypoxia-induced (*Lower*) clusters. Sample names correspond to the promoters used for *FLAG-RPL18* expression (Table 1). RT, root tip; R, root; S, shoot; C, control; H, 2-h hypoxia. Fig. S10 in *SI Appendix* shows an expanded panel *D*.

tions provides strong evidence for the capture of mRNAs from the targeted cell types (Dataset S4, sheet *f*).

Fuzzy *k*-means clustering also resolved distinctions between the translatomes of the root tip, whole root, or regions differentiated by promoter expression (Fig. 2*A*; Dataset S3; Fig. S5 in *SI Appendix*). Both *pWOL* and *pSHR* are reportedly expressed in the pericycle and vasculature (25, 26), but *pSHR* is inactive in the phloem CC and less active in mature vasculature (27). We detected lower FLAG-GFP-RPL18 fluorescence in the pericycle with *pSHR* than with *pWOL* (Fig. S1*B* in *SI Appendix*). Consistently, the *pWOL* and *pSHR* populations were highly overlapping (cluster 41) but included independently enriched transcripts (i.e., *pWOL* clusters 18 and 56). In the whole root samples, *pSHR*, *pWOL*, *p35S*, and *pRPL11C* mRNAs overlapped, as predicted from the distribution of GFP-RPL18 directed by these promoters (Fig. S1*B* in *SI Appendix*). The shared mRNAs, for example cluster 53, encoded proteins involved in secondary cell wall synthesis (4.24*E*-04). On the other hand, endodermal (*pSCR*) mRNAs were enriched for proteins involved in fatty acid biosynthesis (2.89*E*-08), response to oxidative stress (1.89*E*-02) and genes necessary for suberin biosynthesis (At3g11430 and At5g58860) (28, 29) (clusters 19 and 25; Fig. 2*A*; Fig. S5*B* in *SI Appendix*), consistent with the boundary layer function of endodermis. The DEG and clustering analyses exposed notable distinction between the mRNAs enriched in the apical (*pCO2*, clusters 58, 59, and 10) versus elongation/maturation (*pPEP*, clusters 8, 11, 13, 15, 26, and 29) zones of the cortex (Fig. 2*A*; Fig. S8 in *SI Appendix*). For example, *pCO2* mRNAs were enriched for the binding (7.72*E*-05)

and transport of lipids (4.74*E*-02), whereas *pPEP* mRNAs were enriched for proteins involved in nonphotosynthetic primary and secondary metabolism (i.e., cluster 8, catalytic activity, 7.78*E*-09) and vacuolar membrane (cluster 26, 7.27*E*-04). Thus, these cortex specific promoters can be used to isolate spatially and molecularly distinct translatomes.

Brief Hypoxic Stress Remodels Translatomes at the Global and Cell-Specific Level. We showed previously that hypoxia, which deprives cells of oxygen required for aerobic metabolism and carbon dioxide needed for photosynthesis, selectively limits protein synthesis as a means of energy conservation in *Arabidopsis* seedlings (13). In that study, brief hypoxia (2 h) significantly reduced 4.2% of the mRNAs in the transcriptome, concomitant with reduction of 63% of the translatome, primarily because of inhibition of initiation of translation and transient mRNA sequestration. Here, the seedling response to hypoxia was further scrutinized at the organ-, region-, and cell-specific levels. We found that seedlings exposed to hypoxia showed a greater reduction in polysomes in the root (27%) than the shoot (14%). This was coincident with a more severe decline in ATP content and more dramatic remodeling of the translatome in the root than the shoot (Fig. 3). All 19 translatomes and three transcriptomes surveyed displayed significant elevation of 49 transcripts in response to the stress (Dataset S5). Not unexpectedly, these ubiquitously hypoxia-responsive mRNAs encode proteins associated with reconfiguration of metabolism to augment substrate level ATP production and fermentation [i.e., SUS4, sucrose

Fig. 4. Plasticity in transcription factor mRNA abundance in translatomes. (*A*–*C*) Cell-specific TFs. (*A*) Numbers of genes belonging to a TF family that are significantly enriched in at least 1 mRNA population. Gene counts were made on the basis of Dataset S2, sheet *a*. (*B*) Level of expression of 3 TF families in 7-d-old seedlings under control and hypoxia stress. Data organized by hierarchical clustering in the TIGR MEV program (MEV). Values are scaled RMA normalized data, with control (*Left*) and hypoxia (*Right*) data shown in pairs for each mRNA population. (*C*) Display of absolute expression values for ATMYB93 (At1g34670) in the root. (*D*–*F*) Hypoxia-induced TFs. (*D*) Numbers of genes belonging to TF families that are significantly induced by hypoxia in at least one mRNA population. Gene counts were made on the basis of Dataset S5, sheet *b*. Others, TF families with fewer than five DEGs. (*E*) Level of induction of three TF families under hypoxia stress. Data organized by hierarchical clustering. Values are signal-log-ratios of hypoxic versus control data for each mRNA population. (*F*) Display of absolute expression values for ERF71 (At2g47520) in the root.

synthase (At3g43190); *PFK4*, ATP-dependent-phosphofructokinase (At4g32840); *PDC1* and *PDC2*, pyruvate decarboxylase (At4g33070 and At5g54960); alcohol dehydrogenase (At1g77120); alanine aminotransferase (At1g17290); and putative lactate transporter (At2g34390)] (Fig. S9*A* in *SI Appendix*) (13). Notably, >50% of these mRNAs encode proteins of no known biological function, emphasizing that the core response involves poorly understood processes.

To explore the organ and cell-specific response to hypoxia, fuzzy *k*-means clustering was performed on the 6,416 mRNAs that displayed a significant change in 1 or more samples under hypoxia (>2-fold change; FDR < 0.01) (Dataset S6). The output exposed variation in adjustments of translatome populations at the global-, regional-, or cell-specific level (Fig. 3*D*; Fig. S10*A* in *SI Appendix*). The observed changes could reflect regulation of 1 or more of the following processes: transcription, mRNA turnover, or translation. However, a marked decline in ribosome-associated mRNAs was expected for a large proportion of the transcriptome because hypoxia increases the selectivity of translational initiation to conserve energy (Figs. S9*B* and S10*B* in *SI Appendix*) (13).

The reduction in cell-specific-enriched mRNAs was a pronounced feature of the seedling hypoxia response. This decline was more extreme in the root tip and root than the shoot (i.e., 41% and 21% of *pSCR*-enriched mRNAs were reduced in root tip and whole root, respectively, whereas 17% and 2.5% of *pSUC2*-enriched mRNAs were reduced in root and shoot, respectively; Dataset S2, sheet *c* and Dataset S5, sheet *h*). At the regional level, mRNAs associated with cell-wall organization and biogenesis and trichoblast differentiation were excluded from ribosomes in the root tip (cluster 54; Fig. S10*B* in *SI Appendix*). At the cell-specific level, translation of mRNAs associated with diverse specialized processes was repressed [i.e., cluster 72, stele, auxin biosynthesis (4.82*E*-04); cluster 11, endodermis, fatty acid metabolism (1.75*E*-06); cluster 70, mature cortex, glycolsyl transferase activity (6.33*E*-03); cluster 5, shoot epidermis, response to auxin (3.31*E*-07); cluster 61, guard cell, protein phosphatases associated with stomatal activity (2.68*E*-03); Fig. S10*B* in *SI Appendix*]. These findings indicate that production of proteins associated with specialized processes in specific cell populations is limited during the stress.

In addition to ubiquitously hypoxia-induced mRNAs (i.e., 49 core-induced mRNAs in Dataset S5 and cluster 55 in Fig. 3*C*; Fig. S10*C* in *SI Appendix*), there were transcripts induced at the organ- or cell-specific level. Root cell populations showed a more dramatic increase in the ubiquitously induced mRNAs encoding enzymes responsible for increased glycolysis and fermentation, whereas shoots showed a high increase in mRNAs involved in synthesis of galactolipid and stress responses (i.e., clusters 3, 41, 69; Fig. S10*C* in *SI Appendix*). The stronger induction in roots of mRNAs that promote anaerobic metabolism is consistent with the proposal that limited production of ATP by chloroplasts continues in photosynthetic cells during oxygen deprivation (30). Other mRNAs exhibited induction in subsets of organ cells (cluster 93, root stele, auxin-responsive, 1.66*E*-03), or specific cell populations [cluster 8, mature root cortex, glutathione-S-transferases (7.38*E*-05); cluster 46, shoot plastid-containing cells, transoctaprenyltrantransferase (8.05*E*-05)] (Fig. 3*D*; Dataset S6; Fig. S10*C* in *SI Appendix*). Here, again the phloem CC mRNA population provides an interesting example. In both the root and shoot this translatome maintained higher levels of hypoxia-induced mRNAs under control growth conditions (*pSUC2*, 22 shoot and 27 root hypoxia-induced mRNAs; Dataset S2, sheet *c* and Dataset S5, sheet *m*) and strongly induced mRNAs associated with the response to heat shock [clusters 44 and 47; 15 HSPs, TFs HSFA6b (At3g22830), HSFA2 (At2g26150)]. The stress-induced HSP mRNAs were also pronounced in the root, with at least 1 member of the 17-, 23-, 70-, 90-, and 100-kDa HSP families strongly upregulated in each cell population assayed (Fig. S11 in *SI Appendix*). Because seedling survival is enhanced when a brief heat shock precedes severe oxygen deprivation (31), the hyperenrichment of HSP mRNAs in phloem CC could provide additional resilience to cells that are constitutively oxygen deficient.

Differential Expression of Transcription Factor Family Members. The translatome dataset can be used to uncover intricate developmental and environmental regulation of proteins encoded by complex families, such as the ≈1,600 putative TFs represented on the ATH1 array (Fig. 4*A*; Figs. S12*A* and Fig. S13 in *SI Appendix*). Members of the MYB, bHLH, C2H2, and homeobox families showed the greatest cell-specific enrichment under control conditions (Fig. 4 *B* and *C*). For example, G2-like and C2C2-DOF factors were overrepresented in phloem CC (*pSUC2*) mRNAs (5.79*E*-07 and 1.84*E*-

Vertical PLANT BIOLOGY label and PNAS side text

PLANT BIOLOGY

06, respectively) whereas R2-R3-type MYB TF mRNAs were abundant in root *pSCR* and shoot *pCER5* mRNAs (Fig. S12*B* in *SI Appendix*). This latter enrichment was accompanied by an over-representation of the MYB4 binding in the 5′ flanking regions of *pSCR* and *pCER5*-enriched genes (Fig. S12*D* in *SI Appendix*).

Overall, hypoxia dramatically remodeled the TF mRNA translatome (Fig. 4*B*; Fig. S14*A* in *SI Appendix*). This included marked elevation of specific TF mRNAs in nearly all families, with increases most pronounced for WRKY and ethylene-responsive factor (AP2-EREBP/ERF) TFs (Fig. 4 *D–F*; Dataset S5; Fig. S14*B* in *SI Appendix*). The increase in ERF71 and ERF73 (At2g47520 and At1g72360) and WRKY70 (At3g56400) mRNAs was ubiquitous, whereas other members of these and other TF families showed more regional and cell-specific regulation (Figs. S13 *A* and *B* and S14*B* in *SI Appendix*). The elevation in mRNAs encoding WRKYs was accompanied by an overrepresentation of W-box binding sites in the 5′ flanking region of hypoxia-responsive genes (Fig. S13*D* in *SI Appendix*). The remodeled TF translatomes also included decreased mRNA abundance or translation of TFs enriched in specific cell populations (i.e., AtMYB93) (Fig. 4 *C* and *F*; Fig. S14*A* in *SI Appendix*). The response of *Arabidopsis* roots to salt and iron stress also included global and cell-specific alterations in steady-state levels of TF mRNAs (6), but these stresses invoked more pronounced cell-specific responses than hypoxia. The limited cell-specific response to hypoxia most likely reflects the need for a metabolic acclimation strategy that enables endurance of a severe energy crisis regardless of cell identity.

Conclusions

We present here the first large-scale compendium of the subpopulation of cellular mRNAs obtained by immunoprecipitation of ribosomes across photosynthetic and nonphotosynthetic cell types of *Arabidopsis* seedlings. Two benefits of the immunopurification of ribosomes are that cell-specific mRNA populations can be obtained from cyropreserved tissue and translatomes provide a better estimate of protein synthesis than the transcriptome. The study determined that cells of different identity have distinct translatomes but responded in a unified manner to hypoxia by promoting translation of a core group of mRNAs that facilitate acclimation. Superimposed on the core response were regional and cell-specific adjustments in mRNAs that encode proteins anticipated to affect stress tolerance, metabolism, and development. This cell-specific gene expression dataset is a valuable resource for plant biologists. For example, the TF family member mRNAs in the individual translatomes expose a signature of cell identity, providing prime targets for future study of networks that regulate development and environmental responses.

Materials and Methods

Plant Growth and Treatment. Transgenic *A. thaliana* (Col-0) lines containing a *promoter:FLAG-RPL18* or *promoter:FLAG-GFP-RPL18* construct were produced and characterized as described in the *SI Appendix*. For experiments, seeds were grown vertically on the surface of solid MS media (0.43% (wt/vol) Murashigi Skoog salts (Sigma), 0.4% (wt/vol) phytagel (Sigma), 1% (wt/vol) sucrose, pH 5.7), under long day conditions (16 h light at ≈80 μmol photons m^{-2} s^{-1}/8 h darkness) at 23 °C. Hypoxia stress (HS) was imposed after the end of the light period after 7 d, by gassing in chambers with 99.99% (vol/vol) argon for 2 h at <5 to 7 μmol photons m^{-2} s^{-1} light (13) (see *SI Appendix* for details). Control samples were maintained under the same condition in chambers open to air. For the root tip experiment set, the apical 1 cm of the root was harvested. In another experiment set, the entire root below the hypocotyl–root junction and the shoot were separately collected.

Immunopurification of Ribosomes, Microarray Hybridizations, and Expression Data Analysis. The immunopurification of ribosomes from *p:FLAG-RPL18* lines (individual 60S subunits, ribosomes, and polysomes) was accomplished as described earlier (13, 17). The yield of RNA obtained by immunoprecipitation of ribosome complexes varied from 1 ng/mL tissue for *pKAT:FLAG-RPL18* to 1 μg/mL tissue for *p35S:FLAG-RPL18*. Total RNA was extracted from an aliquot of the same cell lysates. Detailed procedures are given in the *SI Appendix*. After quality assessment, the RNA probes were prepared using two linear rounds of target amplification and hybridized against the *Arabidopsis* ATH1 Genome Array (GeneChip System, Affymetrix) chips as detailed in the *SI Appendix*. Analysis of expression data was as described in the *SI Appendix*.

1. Birnbaum K, et al. (2003) A gene expression map of the Arabidopsis root. *Science* 302:1956–1960.
2. Nawy T, et al. (2005) Transcriptional profile of the Arabidopsis root quiescent center. *Plant Cell* 17:1908–1925.
3. Zhang C, Barthelson RA, Lambert GM, Galbraith DW (2008) Global characterization of cell-specific gene expression through fluorescence-activated sorting of nuclei. *Plant Physiol* 147:30–40.
4. Brady SM, et al. (2007) A high-resolution root spatiotemporal map reveals dominant expression patterns. *Science* 318:801–806.
5. Jiao Y, et al. (2009) A transcriptome atlas of rice cell types uncovers cellular, functional and developmental hierarchies. *Nat Genet* 41:258–263.
6. Dinneny JR, et al. (2008) Cell identity mediates the response of Arabidopsis roots to abiotic stress. *Science* 320:942–945.
7. Gifford ML, Dean A, Gutierrez RA, Coruzzi GM, Birnbaum KD (2008) Cell-specific nitrogen responses mediate developmental plasticity. *Proc Natl Acad Sci USA* 105:803–808.
8. Parker R, Sheth U (2007) P bodies and the control of mRNA translation and degradation. *Mol Cell* 25:635–646.
9. Proud CG (2007) Signaling to translation: How signal transduction pathways control the protein synthetic machinery. *Biochem J* 403:217–234.
10. Kawaguchi R, Bailey-Serres J (2002) Regulation of translational initiation in plants. *Curr Opin Plant Biol* 5:460–465.
11. Kawaguchi R, Bailey-Serres J (2005) mRNA sequence features that contribute to translational regulation in Arabidopsis. *Nucleic Acids Res* 33:955–965.
12. Branco-Price C, Kawaguchi R, Ferriera R, Bailey-Serres J (2005) Genome-wide analysis of transcript abundance and translation in Arabidopsis seedlings subjected to oxygen deprivation. *Ann Bot* 96:647–660.
13. Branco-Price C, Kaiser KA, Jang CJ, Larive CK, Bailey-Serres J (2008) Selective mRNA translation coordinates energetic and metabolic adjustments to cellular oxygen deprivation and reoxygenation in *Arabidopsis thaliana*. *Plant J* 56:743–755.
14. Pillai RS, et al. (2005) Inhibition of translational initiation by Let-7 MicroRNA in human cells. *Science* 309:1573–1576.
15. Brodersen P, et al. (2008) Widespread translational inhibition by plant miRNAs and siRNAs. *Science* 320:1185–1190.
16. Halbeisen RE, Gerber AP (2009) Stress-dependent coordination of transcriptome and translatome in yeast. *PLOS Biol* 7:May 5;7(5):e105.

17. Zanetti ME, Chang I-F, Gong F-C, Galbraith DW, Bailey-Serres J (2005) Immunopurification of polyribosomal complexes of Arabidopsis for global analysis of gene expression. *Plant Physiol* 138:624–635.
18. Heiman M, et al. (2008) A translational profiling approach for the molecular characterization of CNS cell types. *Cell* 135:738–748.
19. Winter D, et al. (2007) An ''electronic fluorescent pictograph'' browser for exploring and analyzing large-scale biological data sets. *PLoS ONE* 2:e718.
20. Takahashi H, et al. (2000) The roles of three functional sulphate transporters involved in uptake and translocation of sulphate in *Arabidopsis thaliana*. *Plant J* 23:171–182.
21. Deeken R, et al. (2008) Identification of *Arabidopsis thaliana* phloem RNAs provides a search criterion for phloem-based transcripts hidden in complex datasets of microarray experiments. *Plant J* 55:746–759.
22. Lin MK, et al. (2009) Analysis of the pumpkin phloem proteome provides insights into angiosperm sieve tube function. *Mol Cell Proteomics* 8:343–356.
23. Ohashi-Ito K, Bergmann DC (2006) Arabidopsis FAMA controls the final proliferation/differentiation switch during stomatal development. *Plant Cell* 18:2493–2505.
24. Cominelli E, et al. (2005) A guard-cell-specific MYB transcription factor regulates stomatal movements and plant drought tolerance. *Curr Biol* 15:1196–1200.
25. Mähönen AP, et al. (2000) A novel two-component hybrid molecule regulates vascular morphogenesis of the Arabidopsis root. *Genes Dev* 14:2938–2943.
26. Helariutta Y, et al. (2000) The SHORT-ROOT gene controls radial patterning of the Arabidopsis root through radial signaling. *Cell* 101:555–567.
27. Sena G, Jung JW, Benfey PN (2004) A broad competence to respond to SHORT ROOT revealed by tissue-specific ectopic expression. *Dev* 2131:2817–2826.
28. Beisson F, Li Y, Bonaventure G, Pollard M, Ohlrogge JB (2007) The acyltransferase GPAT5 is required for the synthesis of suberin in seed coat and root of Arabidopsis. *Plant Cell* 19:351–368.
29. Höfer R, et al. (2008) The Arabidopsis cytochrome P450 CYP86A1 encodes a fatty acid omega-hydroxylase involved in suberin monomer biosynthesis. *J Exp Bot* 59:2347–2360.
30. Mustroph A, et al. (2006) Organ specific analysis of the anaerobic primary metabolism in rice and wheat seedlings II: Light exposure reduces needs for fermentation and extends survival during anaerobiosis. *Planta* 225:139–152.
31. Banti V, et al. (2008) Heat acclimation and cross-tolerance against anoxia in Arabidopsis. *Plant Cell Environ* 31:1029–1037.
32. Horan K, et al. (2008) Annotating genes of known and unknown function by large-scale coexpression analysis. *Plant Physiol* 147:41–57.